

Supplement of Atmos. Chem. Phys., 17, 10733–10741, 2017
<https://doi.org/10.5194/acp-17-10733-2017-supplement>
© Author(s) 2017. This work is distributed under
the Creative Commons Attribution 3.0 License.



Supplement of

Direct molecular-level characterization of different heterogeneous freezing modes on mica – Part 1

Ahmed Abdelmonem

Correspondence to: Ahmed Abdelmonem (ahmed.abdelmonem@kit.edu)

The copyright of individual parts of the supplement might differ from the CC BY 3.0 License.

Abbreviations

SHG: second-harmonic generation, SFG: sum-frequency generation, IMG: index-matching gel, TIR: total internal reflection, and RH: relative humidity

SFG and SHG: Theoretical background

SFG and SHG are highly sensitive nonlinear optical probes of surfaces and interfaces where light is generated at a frequency equals to the sum of frequencies of two incident optical fields. The basic theory of SHG and SFG has been described elsewhere (Bain, 1995; Eisenthal, 1996; Richmond et al., 1988; Shen, 1989a; Shen, 1989b; Shen, 1994; Shen and Ostroverkhov, 2006) and will not be repeated here. However, a brief background will be given here. SFG/SHG signal is generated when the incident beams are spatially and temporally overlapped at a point of broken inversion-symmetry (e.g. an interface between two isotropic media). The experiments are usually carried out with definite polarization combinations of incident and generated beams. Such experiments are rich of information, particularly about concentrations and orientations of the entities which contribute to the signal. Unlike SHG, SFG can specify the different entities from their resonance frequencies. SHG and SFG have been used to probe the aqueous/air, aqueous/solid and solid/air interfaces. The overall signal strength depends on 1) intensity and polarization of the incident beams, 2) the optical properties of the media at the interface manifested in the Fresnel factors and 3) the concentrations and orientations of the molecules and the response of the existing dipoles at the interface.

Generally the SFG signal, of frequency $\omega_{SF} = \omega_v + \omega_{IR}$, generated at the interface, Figure (S1), is given as below:

$$I(\omega_{SF}) \propto |L(\omega_{SF}) \chi^{(2)} L(\omega_v) \cdot L(\omega_{IR})|^2 I_v I_{IR} \quad (1)$$

where, $L(\omega_i)$ is the nonlinear Fresnel factor at ω_i and $\chi^{(2)}$ is the second order nonlinear hyperpolarizability tensor. ω_v and ω_{IR} are the frequencies of the incident beams. In SHG, the two incident frequencies are equal. Polarization dependent measurements probe specific tensor element of the hyperpolarizability tensor and yield detailed information about the degree of ordering and angular orientation of the molecules (Abdelmonem, 2008; Shen, 1989a; Shen, 1989b; Jang et al., 2013; Rao et al., 2003; Zhuang et al., 1999; Fordyce et al., 2001; Goh et al., 1988; Luca et al., 1995).

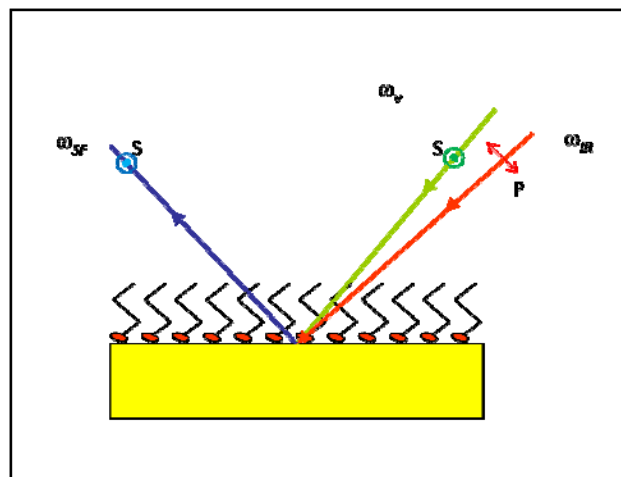


Figure S1: Simple scheme of SFG generation in co-propagating geometry. S and P indicate light polarized light perpendicular and parallel to the plane of incidence respectively.

Data acquisition and Fresnel factors correction (SHG)

- Data acquisition

During the SHG experiments the signal was collected, averaged and stored as a function of the state of condensation, deposition, freezing, or formation of bulk. These are the data points plotted in Figs. 3 and 4 in the manuscript. Only for Fig. 5 the data was recorded as a function of time to report on the detected transient ice formed upon immersion freezing. Figure S2, shows some screen shots of typical SHG signal and temperature changes in time, and shows the points where the signal was collected and averaged for Figs. 3 and 4.

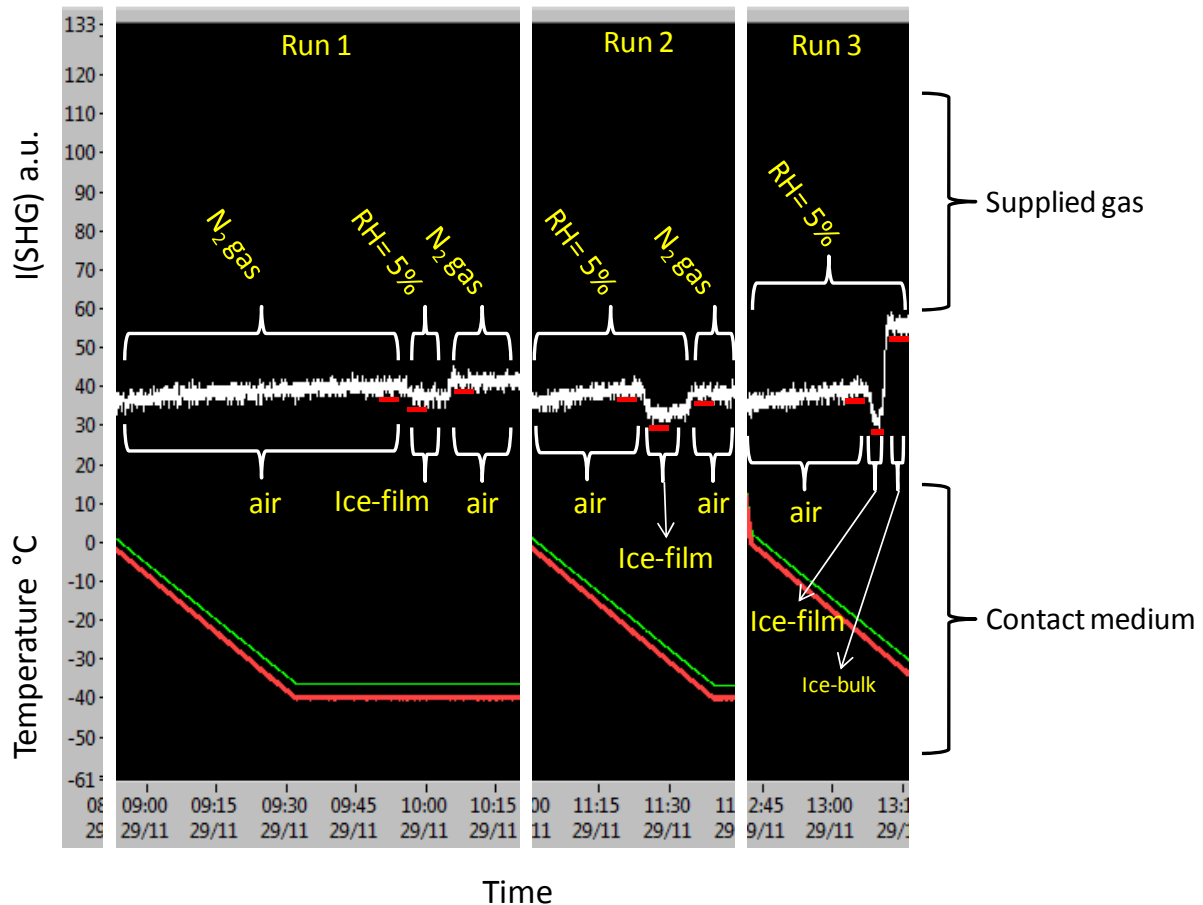


Figure S2: Screen shots of typical signal and temperature changes in time during arbitrary cooling processes. The white line shows raw SHG data. The short red dashes below the SHG data show the points where the signal was collected and averaged. The red and green lines show the temperatures of the sample bottom and sample top respectively.

Figure S2 shows three examples of three arbitrary runs performed on sapphire (only for demonstration purpose):

Run1: The cell was purged continuously with N_2 gas while cooling the sample down to -40. There is a small gradual change in the signal due to the changes in the temperature dependent optical constants. The cell was then purged with humid air which resulted in a formation of an ice-film by deposition. Finally, the cell was purged again with N_2 gas which resulted in sublimation of the ice film.

Run2: The cell was purged with humid air (RH=5%) while cooling the sample down until the formation of an ice film and then the cell was purged by N_2 gas which resulted in film sublimation.

Run3: The cell was purged with humid air (RH=5%) while cooling the sample down until the formation of an ice film. Purging the cell with humid air was continued until the formation of bulk ice. All experiments of deposition freezing were done in a similar way as described above. Figs. 3 and 4 in the manuscript show the averaged signal at each event and the error bars on the figures show the fluctuation in the data points among all repeated experiments.

- *Fresnel factors*

The SHG signal with a frequency $\omega_{SH} = 2\omega_{in}$ under SM polarization, (S-polarized SHG and 45°-polarized incident light), generated from an incoming visible light with a frequency ω_{in} can be described with the equation:

$$S_{SM}(\omega_{SH}) \propto |L_{yy}(\omega_{SH})L_{yy}(\omega_{in})L_{zz}(\omega_{in})\chi_{yyz}^{(2)}|^2 I_{in}^2 \quad (2)$$

where, $L(\omega_i)$ is the nonlinear Fresnel factor at ω_i and $\chi_{yyz}^{(2)}$ is the surface second order nonlinear susceptibility tensor for SM polarisation combination (equivalent to SSP in SFG) (Shen, 1989b; Zhuang et al., 1999) and a measure of the degree of molecular ordering. To obtain the molecular quantity $\chi_{yyz}^{(2)}$ the measured SHG intensities have thus to be normalized to the Fresnel factors which are optical constants dependent. Figure S3 shows the change of Fresnel factors as a function of refractive index in the range of refractive indices covering the involved media in this work. The SHG intensities reported in Figures 3 and 4 in the manuscript are Fresnel corrected and thus directly proportional to $|\chi_{yyz}^{(2)}|^2$.

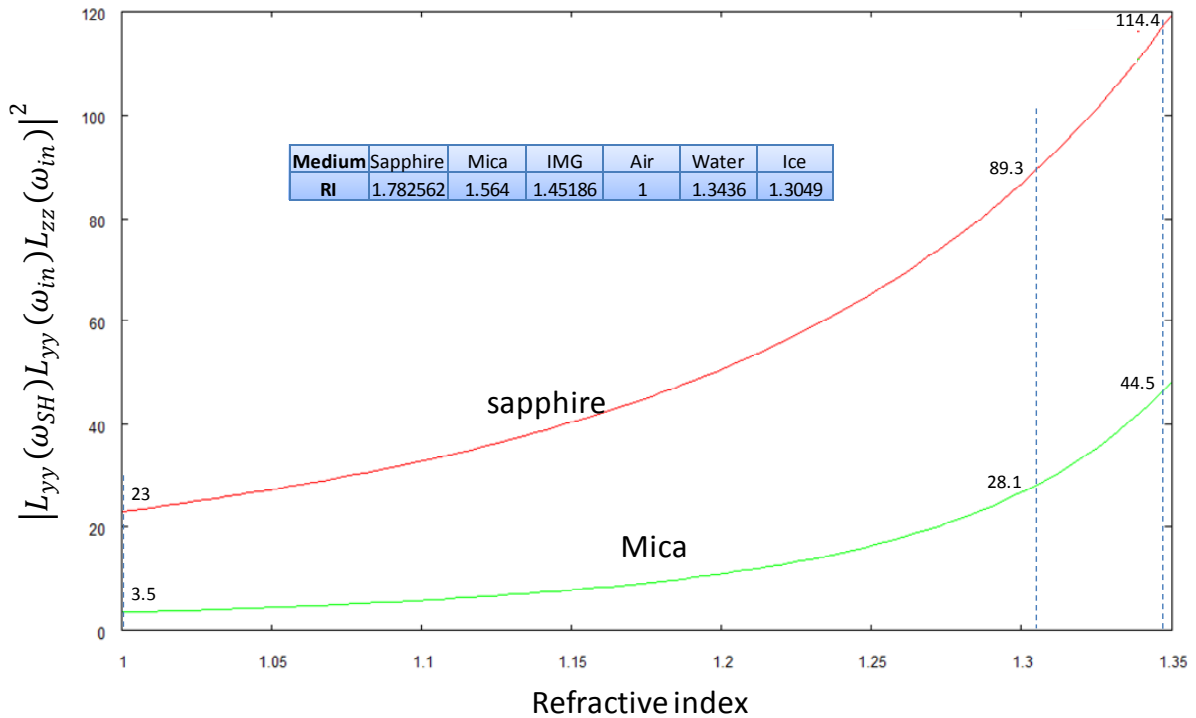


Figure S3: Theoretically calculated Fresnel factors for sapphire-water (red line) and mica-water (green line) interfaces at incident angle of 15° from air to the sapphire prism. Optical geometry can be found in (Abdelmonem et al., 2015; Abdelmonem et al., 2017).

Due to the large difference between the refractive index of air and those of water and ice, Fresnel corrections were made. The Fresnel factors as indicated on Fig. S3 are 3.5, 44.5 and 28.1 for air-, water-, and ice-mica interfaces respectively. Figure S4 shows the data of Fig. 4 before and after Fresnel correction.

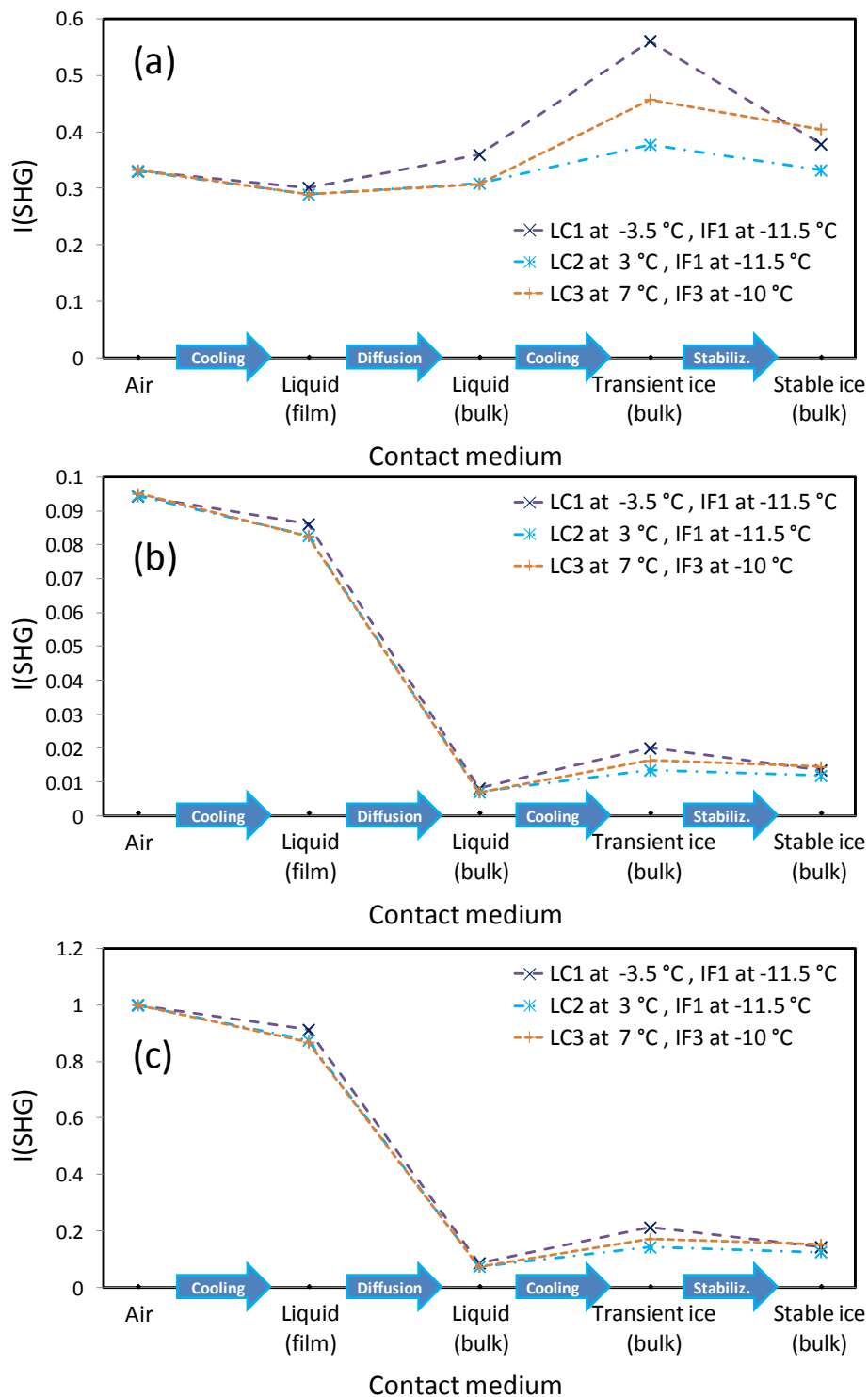


Figure S4. Data in Fig. 4 of the manuscript before and after Fresnel correction. (a) Original data before Fresnel correction, (b) Data after Fresnel correction, and (c) Data after Fresnel correction and normalization to the mica-air signal (= Figure 4 in the manuscript).

The Fresnel factors are expected to change with temperature and hence affect the measured SHG signal. The influence of the temperature dependence of the optical properties of the IMG, sapphire prism and mica on the SHG signal was studied before starting the series of measurements. Figure S5 shows the SHG at mica-N₂ gas interface in the mentioned range of temperatures. There was no significant effect of the changes in the optical properties of these media on the detected signal within the range of freezing temperatures observed in the study.

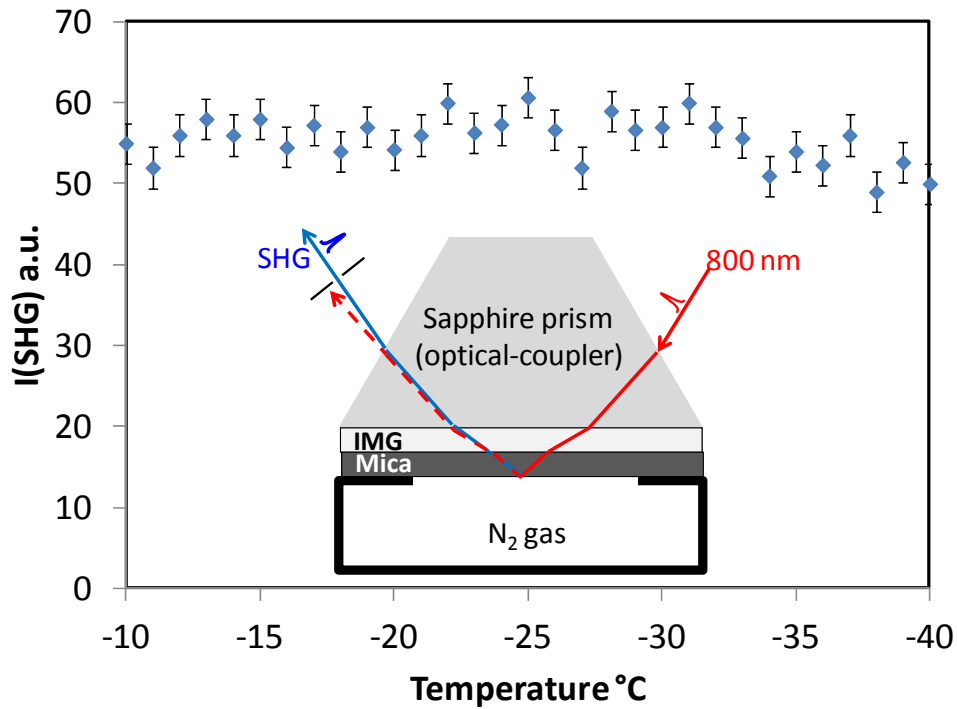


Figure S5: SHG at mica-N₂ gas interface in the range of freezing temperatures observed in the study. The cell, shown in Figure 2, was filled with ultrapure N₂ gas (99.9999 %).

References

- Abdelmonem, A.: Nonlinear optical spectroscopy at the Liquid-/Solid- interface, 1.0, Naturwissenschaften, Mathematik und Informatik, Ruprecht – Karls – Universität, Heidelberg, 2008.
- Abdelmonem, A., Lützenkirchen, J., and Leisner, T.: Probing ice-nucleation processes on the molecular level using second harmonic generation spectroscopy, *Atmos. Meas. Tech.*, **8**, 3519-3526, doi: 10.5194/amt-8-3519-2015, 2015.
- Abdelmonem, A., Backus, E. H. G., Hoffmann, N., Sánchez, M. A., Cyran, J. D., Kiselev, A., and Bonn, M.: Surface charge-induced orientation of interfacial water suppresses heterogeneous ice nucleation on α -alumina (0001), *Atmos. Chem. Phys. Discuss.*, 2017, 1-13, doi: 10.5194/acp-2017-224, 2017.
- Bain, C. D.: Sum-frequency vibrational spectroscopy of the solid/liquid interface, *J. Chem. Soc. Faraday Trans.*, **91**, 1281-1296, doi: 10.1039/ft9959101281, 1995.
- Eisenthal, K. B.: Liquid Interfaces Probed by Second-Harmonic and Sum-Frequency Spectroscopy, *Chem. Rev.*, **96**, 1343-1360, doi: 10.1021/cr9502211, 1996.
- Fordyce, A. J., Bullock, W. J., Timson, A. J., Haslam, S., Spencer-Smith, R. D., Alexander, A., and Frey, J. G.: The temperature dependence of surface second-harmonic generation from the air-water interface, *Mol. Phys.*, **99**, 677-687, doi: 10.1080/00268970010030022, 2001.
- Goh, M. C., Hicks, J. M., Kemnitz, K., Pinto, G. R., Heinz, T. F., Eisenthal, K. B., and Bhattacharyya, K.: Absolute orientation of water molecules at the neat water surface, *J. Phys. Chem.*, **92**, 5074-5075, doi: 10.1021/j100329a003, 1988.
- Jang, J. H., Lydiatt, F., Lindsay, R., and Baldelli, S.: Quantitative Orientation Analysis by Sum Frequency Generation in the Presence of Near-Resonant Background Signal: Acetonitrile on Rutile TiO₂ (110), *J. Phys. Chem. A*, **117**, 6288-6302, doi: 10.1021/jp401019p, 2013.
- Luca, A. A. T., Hebert, P., Brevet, P. F., and Girault, H. H.: Surface second-harmonic generation at air/solvent and solvent/solvent interfaces, *J. Chem. Soc. Faraday Trans.*, **91**, 1763-1768, doi: 10.1039/ft9959101763, 1995.
- Rao, Y., Tao, Y.-s., and Wang, H.-f.: Quantitative analysis of orientational order in the molecular monolayer by surface second harmonic generation, *J. Chem. Phys.*, **119**, 5226-5236, doi: 10.1063/1.1597195, 2003.
- Richmond, G. L., Robinson, J. M., and Shannon, V. L.: Second harmonic generation studies of interfacial structure and dynamics, *Prog. Surf. Sci.*, **28**, 1-70, doi: 10.1016/0079-6816(88)90005-6, 1988.
- Shen, Y. R.: Surface properties probed by second-harmonic and sum-frequency generation, *Nature*, **337**, 519-525, doi: 10.1038/337519a0, 1989a.
- Shen, Y. R.: Optical Second Harmonic Generation at Interfaces, *Annu. Rev. Phys. Chem.*, **40**, 327-350, doi: 10.1146/annurev.pc.40.100189.001551, 1989b.
- Shen, Y. R.: Surfaces probed by nonlinear optics, *Surf. Sci.*, **299**, 551-562, doi: 10.1016/0039-6028(94)90681-5, 1994.
- Shen, Y. R. and Ostroverkhov, V.: Sum-Frequency Vibrational Spectroscopy on Water Interfaces: Polar Orientation of Water Molecules at Interfaces, *Chem. Rev.*, **106**, 1140-1154, doi: 10.1021/cr040377d, 2006.
- Zhuang, X., Miranda, P. B., Kim, D., and Shen, Y. R.: Mapping molecular orientation and conformation at interfaces by surface nonlinear optics, *Phys. Rev. B*, **59**, 12632-12640, doi: 10.1103/PhysRevB.59.12632, 1999.